ГОРЕНИЕ И ПЛАЗМОХИМИЯ 23 (2025) 467–479
Combustion and Plasma Chemistry https:cpc-journal.kz/

МРНТИ 61.69.35, 31.15.33 https://doi.org/10.18321/cpc23(4)467-479

Synergistic Effects of Li^+–Zn^{2+} Hybrid Electrolytes on Corrosion Suppression and Electrochemical Performance of Zn||$LiFePO_4$ Aqueous Batteries

A. Dauletbay[1], B. Myrzakhmetov[1], L. Rakhymbay[1], L. Birles[2], Sh. Bileimova[2], K. Kudaibergenov[3], A. Konarov[4]*

[1]National Laboratory Astana, Nazarbayev University, Kabanbay batyr Ave., 53, Astana, Kazakhstan
[2]Faculty of Chemistry and Chemical Technology, Al-Farabi Kazakh National University, Al-Farabi Ave., 71, Almaty, Kazakhstan
[3]Department of Materials Science, Nanotechnology and Engineering Physics, Satbayev University, Satbaev st., 22, Almaty, Kazakhstan
[4]Department of Chemical and Materials Engineering, School of Engineering and Digital Sciences, Nazarbayev University, Kabanbay batyr Ave., 53, Astana, Kazakhstan

ARTICLE INFO

Received
15.09.2025

Received in revised form
23.10.2025

Accepted
20.11.2025

Keywords:
aqueous zinc-ion batteries; dendrites; lithium iron phosphate; hybrid electrolyte; Zn anode; stripping; plating

ABSTRACT

Aqueous zinc-ion batteries (AZIBs) are promising for safe and sustainable energy storage. However, zinc anode instability, dendrite formation, hydrogen evolution, and corrosion limit long-term performance. This study investigates hybrid electrolytes with varying Zn^{2+} and Li^+ ratios. The 1 M $ZnSO_4$ + 1 M Li_2SO_4 electrolyte demonstrated the lowest corrosion current density (0.00026 $mA \cdot cm^{-2}$), reduced charge transfer resistance (R_{ct} = 8.91 Ω), and stable cycling performance (135-158 $mAh \cdot g^{-1}$ over 50 cycles). Electrochemical and morphological analyses confirmed uniform, dendrite-free Zn deposition. These results highlight the synergistic effect of Li^+–Zn^{2+} hybrid electrolytes in enhancing the performance of AZIB.

1. Introduction

Sustainable, scalable, safe and environmentally friendly electricity storage (ES) systems are crucial to meeting energy demand while reducing carbon emissions. Rechargeable batteries stand out among existing ES technologies due to their high energy density, scalability and adaptability [1-3]. Despite dominating the market for more than thirty years, commercial lithium-ion batteries ace challenges such as limited power density, high cost, and safety issues [4, 5]. Rechargeable aqueous batteries are a promising alternative due to their economy and increased safety associated with the use of non-flammable and environmentally friendly electrolytes. Aqueous zinc-ion batteries (AZIBs) were of great interest due to their high theoretical capacity (820 $mAh \cdot g^{-1}$ or 5855 $mAh \cdot cm^{-3}$), low redox potential of Zn metal anodes (-0.763 V standard hydrogen electrode), as well as their safety. However, uncontrolled Zn chemistry in conventional aqueous electrolytes poses serious challenges, including dendrite formation, hydrogen release, and surface corrosion. These problems gradually degrade the Zn anode/electrolyte interface during battery operation, resulting in uneven Zn deposition, poor reversibility, and eventually cycle failure [8, 11-15]. To overcome these difficulties, much effort has been made to increase the reversibility of the Zn plating/stripping process and extend battery life.

In addition to measures aimed at the anode, hybrid cation strategies (the use of Zn^{2+} in conjunction with a second inorganic cation (Mn^+)) have been a major research area in aqueous zinc-based batteries that offer an additive-free pathway to regulate solution chemistry, suppress side reactions, and maintain indirect stability, as well as enhance interfacial stability while maintaining safety. In recent years, many studies have explored different hybrid systems, and each cation demonstrates unique

---

*Corresponding author: A. Konarov; E-mail address: aishuak.konarov@nu.edu.kz advantages and mechanical roles. For example, Na^+ is the most studied: double cation electrolytes (Zn^{2+} + Na^+) reduce the free activity of water, Zn^{2+} alters solvation membranes and forms stable Zn interphases, improving reversibility and velocity capacity in complete cells with sodium vanadate and phosphate hosts. Hybrid Na–Zn batteries also demonstrated high voltage and long cycle life using NASICON-type cathodes, which confirmed the practicality of Na^+ support [16, 17]. K^+ with a large ionic radius acts as a spectator cation that controls the structure, increases the ionic conductivity, speeds up Zn plating/stripping, and smoothes the Zn surface to suppress dendrites [18].

Multivalent ions provide additional complexity and advantages. Mg^{2+}, due to its strong ion pairing with sulfate and unique hydration behavior, stabilizes vanadate cathodes in $ZnSO_4$ – $MgSO_4$ hybrids by facilitating dissolution-recombination processes and reducing active material loss; simulations confirm the ability of Mg^{2+} to disrupt Zn^{2+} associations in mixed sulfates [19, 20]. Similarly, Ca^{2+} offers a small Stokes radius and a strong electrostatic screening at the Zn interface, allowing for fast ion transport and dendrite suppression in full cels based on NASICON [21]. In high-valence regimes, Al^{3+} co salts can extend the aqueous stability window, reduce the formation of the main zinc salt, and stabilize layered vanadates, although careful optimization is required to avoid cathodic side reactions [22]. Among them, Li^+ ions are particularly interesting due to their small ionic radius and high hydration energy, which allows them to modify the structure of Zn^{2+} solution and improve interfacial ion transport. Despite this potential, comprehensive studies that combine linear polarization resistance (LPR), cyclic voltammetry (CV), electrochemical impedance spectroscopy (EIS), charge-discharge cycling, and morphological analysis (SEM/EDS) of $ZnSO_4$ – Li_2SO_4 hybrid electrolytes are still pending.

Overall, these findings suggest that hybrid Zn systems are not a one-size-fits-all approach but rather a universal design space where each cation brings unique advantages – from interfacial stabilization and dendritic control to ionic conductivity and cathode compatibility. Recent reviews suggest that dual-cation designs are a promising, scalable strategy for advancing aqueous Zn metal batteries toward high-rate, long-life, and safe energy storage [23].

In addition to these anode central pathways, the combined cathode and electrolyte design further increases the performance envelope. The choice of a robust polyanion cathode such as $LiFePO_4$ (LFP) decouples the cathode kinetics from slow Zn^{2+} intercalation: operando analysis of hybrid Zn‖LFP cells shows Li^+ (de)insertion only at the LFP cathode, while there is a high barrier Zn^{2+} intercalation pathway and accelerated charge transfer kinetics during plate transition [24]. In this hybrid regime, bi-salt aqueous electrolytes combining $ZnSO_4$ nd Li_2SO_4 offer practical advantages: Li^+ reduces interfacial resistance and stabilizes the electrode/electrolyte interfaces in the LFP, while the Zn^{2+} metal is controlled at the anode; the bi-salt environment has provided improved reversibility and rate capability in several hybrid chemistries and is widely recommended in recent electrolyte reviews for Zn systems in water [25, 26]. In addition to kinetics, the olivine framework of LFP exhibits high aqueous stability compared to layered/spinel oxides (e.g., LMO/NMC), which suffer from Mn dissolution or structural degradation under aqueous conditions; conversely, the PO_4^{3-} framework in LFP provides high lattice strength and facilitates degradation under water exposure [27].

LFP interface engineering (e.g., AlF_3 nanocoatings) further suppresses parasitic passivation in aqueous media and reduces interfacial resistance, extending cycle life – an approach that is readily transferable to Zn–Li hybrid cells [28]. On the electrolyte side, concentrated Li^+ + Zn^{2+} aqueous electrolytes have been shown to stabilize phosphate cathodes (e.g., $Li_3V_2(PO_4)_3$) against voltage decay and capacity loss. Extensive studies in ZIB chemistry also support Li^+-based hybrid electrolytes as an effective way to combine safety with high-rate cycling [24, 25]. Finally, $ZnSO_4$ + Li_2SO_4 based gel/antifreeze hydrogel electrolytes suppress hydrogen evolution and Fe dissolution, inhibit Zn dendrites, and maintain reversibility at subzero temperatures, extending the operating window of Zn‖LFP cells to wide-temperature applications [29]. The LFP + ($ZnSO_4$ – Li_2SO_4) + Zn triad offers a non-flammable, structurally robust, and kinetically flexible platform that complements advances oriented to anodes and enables long lifetime, high rate, and potentially wide temperature operation of aqueous Zn ions [24-27, 30-32].

The aim of this work is to systematically investigate the synergistic effect of Li^+ in $ZnSO_4$-based aqueous electrolytes. We aim to demonstrate how the $ZnSO_4$ – Li_2SO_4 mixture affects corrosion resistance, charge transfer resistance, cycling stability, and surface morphology of the zinc anode, thus identifying an optimized electrolyte formulation for hybrid aqueous zinc-ion batteries.

2. Methods and materials

Zn foil (Zn, thickness 0.2 mm), Zinc sulfate heptahydrate ($ZnSO_4{\cdot}7H_2O$, 99.0%), Lithium sulfate monohydrate ($Li_2SO_4{\cdot}H_2O$, 99.0%) was purchased from Sigma-Aldrich. All the reagents used were commercially available without further purification. $LiFePO_4$ (Hohsen, Japan), 10 wt% polyvinylidene fluoride (PVdF, Kynar, HSV900) as a binder and 10 wt% ethynylene black (Co., Japan).

Blank electrolytes were synthesized by dissolving $ZnSO_4{\cdot}7H_2O$ and $Li_2SO_4{\cdot}H_2O$ in deionized water to adjust the concentration of 2M $ZnSO_4$ and 2M Li_2SO_4. The solution was then stirred 2 h at room temperature. Various electrolyte mixtures were prepared with different ratios of zinc and lithium aqueous solutions, respectively (Zn:Li) 2:0; 1.5:0.5; 1:1; 0.5:1.5; 0:2. The obtained clear electrolyte solutions were directly used for cell assembly without any pretreatment process.

$LiFePO_4$ positive electrodes were prepared by mixing 80 wt% $LiFePO_4$ (Hohsen, Japan), 10 wt% polyvinylidene fluoride as a binder and 10 wt% ethynylene black. CR2032-type coin cells were used for main battery testing. They were constructed using cut LFP cathode disks (1.6 cm in diameter), zinc disks (1.6 cm in diameter) as the anode, with an AGM separator (1.9 cm in diameter) between the two electrodes. The appropriate electrolyte was then added and the coin cells were compressed to 750 psi using a hydraulic crimping machine to seal them shut. Galvanostatic charge/discharge tests were performed with a Neware series 3000 battery tester (BTS, 5 V,10 mA) using CR2016 type coin cells at room temperature. The Tafel plots were performed on a three-electrode system with Zn foil as the working electrode, Pt foil as the counter electrode, and Ag/AgCl as the reference electrode at a scan rate of 1.0 mV/s within EOCP ± 150 mV conducted on an Autolab PGSTAT302N. Cyclic voltammetry (CV) tests of the Zn‖$LiFePO_4$ full cells were performed at a scan rate of 1.0 $mV{\cdot}s^{-1}$ from 0.2 to 1.6 V and electrolyte ionic conductivity was measured by electrochemical impedance spectroscopy (EIS) in a frequency range of 100 kHz-0.01 Hz within Zn‖$LiFePO_4$ coin cells on a Bio-Logic VMP3 electrochemical workstation. The morphology, phases, and chemical states of the Zn anode surface after charge/discharge process were characterized by a scanning electron microscope (SEM, Joel).

3. Results

Effect of Electrolyte Composition on Zinc Corrosion and Hydrogen Gas Evolution. In zinc-based aqueous battery systems, the evolution of the hydrogen gas at the anode is the main parasitic reaction that accompanies zinc corrosion. This process reduces the coulombic efficiency, consumes active electrode material, and accelerates pH drift and internal pressure build-up – all of which negatively affect the long-term performance and safety of the battery. To better understand how electrolyte composition affects these degradation mechanisms, linear polarization measurements were performed using five different combinations of $ZnSO_4$ and Li_2SO_4 concentrations.

Figure 1 shows the linear polarization plots for five different electrolyte compositions, and the corresponding corrosion parameters are summarized in Table 1. Of all conditions tested, the binary electrolyte containing 1M $ZnSO_4$ and 1M Li_2SO_4 showed the lowest corrosion current density (0.00026 $mA{\cdot}cm^{-2}$). This very low value indicates that this composition is highly effective in passivating the zinc surface and strongly suppressing the hydrogen evolution reaction (HER). Although the corrosion potential E_{corr} in this system (-0.9978 V) is not the most positive, the sharp decrease in the corrosion current density j_{corr} clearly indicates that electrochemical side reactions in the anode are minimized under these conditions.

In contrast, the addition of Li^+ at other ratios had mixed effects. The 1.5 M $ZnSO_4$: 0.5 M Li_2SO_4 mixture resulted in a significant increase in the corrosion current (1.15 $mA{\cdot}cm^{-2}$), indicating increased zinc dissolution and accelerated HER.

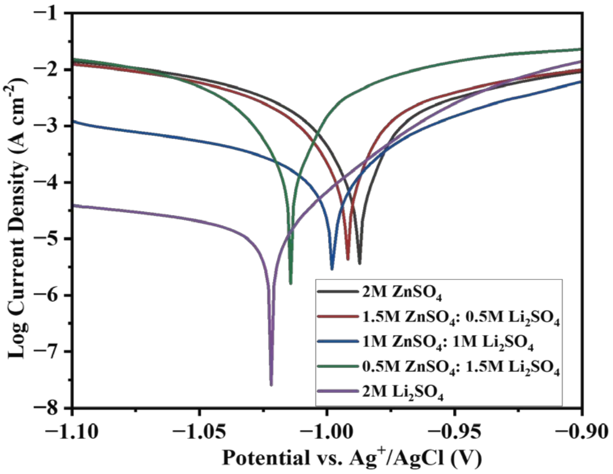

Fig. 1. Tafel plots in various electrolyte solutions using a three-electrode system.

Table 1. Summary of corrosion potentials and currents from linear polarization experiments on zinc in different concentrations ratio $ZnSO_4$ and Li_2SO_4

Condition	Corrosion Potential [E vs. $Ag^+/AgCl$]	Corrosion Current Density [$mA \cdot cm^{-2}$]
2 M $ZnSO_4$	-0.9849	0.21
1.5 M $ZnSO_4$: 0.5 M Li_2SO_4	-0.9921	1.15
1 M $ZnSO_4$: 1 M Li_2SO_4	-0.9978	0.00026
0.5 M $ZnSO_4$: 1.5 M Li_2SO_4	-1.0143	1.94
2 M Li_2SO_4	-1.0219	0.015

Similarly, the composition of 0.5 M $ZnSO_4$: 1.5 M Li_2SO_4 also showed a high corrosion current (1.94 $mA \cdot cm^{-2}$), confirming that the excess lithium-ion concentration destabilizes the zinc interface. In particular, the control sample with only 2 M $ZnSO_4$ showed an average j_{corr} of 0.21 $mA \cdot cm^{-2}$, while the Li_2SO_4 electrolyte alone (2 M) showed a low corrosion current (0.015 $mA \cdot cm^{-2}$), but this system lacks zinc and is not practical.

These results indicate that a 1:1 ratio of Zn^{2+} to Li^+ creates an ideal balance that stabilizes the zinc anode and significantly reduces corrosion. This suppression of HER is beneficial not only for extending cycle life but also for reducing the formation of zinc dendrites, which are often exacerbated by local pH shifts and uneven current distribution associated with rapid gas evolution. Although Tafel analysis does not directly demonstrate dendrite formation, the low current density and small overpotentials observed in this system indicate a reduced risk of localized high-current spots that typically initiate dendrite growth. Additionally, the sharp increase in j_{corr} in these cases may be attributed to localized pH changes and enhanced water activity, which accelerate parasitic reactions. The 2 M Li_2SO_4 system, although showing low j_{corr}, lacks Zn^{2+} and is not suitable for practical use.

The cyclic voltammetry (CV) measurements were conducted to evaluate the electrochemical reversibility and stability of zinc deposition/stripping in different $ZnSO_4$ – Li_2SO_4 electrolytes. The extracted electrochemical parameters from Fig. 2 (Supplementary, Figs. S1a,b,c,d) including anodic peak potential (E_{pa}), cathodic peak potential (E_{pc}), peak-to-peak separation (ΔE_p), and the anodic-to-cathodic current ratio (I_{pa}/I_{pc}) are summarized in Table 2.

The peak-to-peak separation values (ΔE_p) for all Zn-containing electrolytes were in the range of 0.21-0.24 V, indicating a quasi-reversible electrochemical process. Among them, the 1 M $ZnSO_4$ + 1 M Li_2SO_4 electrolyte had the most favorable characteristics: a relatively balanced anodic-cathode peak current ratio ($I_{pa}/I_{pc} \approx 1.41$), indicating an improved reversibility of the zinc plating/stripping process. In contrast, binary electrolytes with asymmetric Zn^{2+}:Li^+ ratios (1.5 M $ZnSO_4$ + 0.5 M Li_2SO_4 and 0.5 M $ZnSO_4$ + 1.5 M Li_2SO_4) showed high current ratios ($I_{pa}/I_{pc} \approx 1.5$-1.6) between anodic and cathodic processes, which could be related to side reactions or partial passivation of the electrode. The 2 M $ZnSO_4$ electrolyte itself also showed acceptable performance ($\Delta E_p = 0.218$ V), but its I_{pa}/I_{pc} ratio was somewhat higher (1.52), indicating a lower ideal reversibility compared to the equimolar Zn^{2+}/Li^+ system. The 2 M Li_2SO_4 electrolyte, on the other hand, showed a low electrochemical activity of $I_{pa}/I_{pc} = 0.68$, indicating that there were not enough Zn^{2+} ions for reversible zinc deposition/stripping. This result confirms that Li_2SO_4 alone cannot support effective operation of Zn-ion batteries. It also highlights the necessity of Zn^{2+} in the electrolyte to enable reversible redox behavior. This confirms that Li_2SO_4 alone does not

Table 2. Electrochemical parameters obtained from CV analysis in different electrolytes

Electrolyte	E_{pa} (V)	E_{pc} (V)	ΔE_p (V)	I_{pa}/I_{pc}
2M $ZnSO_4$	1.252	1.034	0.218	1.52
1.5M $ZnSO_4$ + 0.5M Li_2SO_4	1.304	1.094	0.210	1.58
1M $ZnSO_4$ + 1M Li_2SO_4	1.334	1.098	0.236	1.41
0.5M $ZnSO_4$ + 1.5M Li_2SO_4	1.358	1.118	0.240	1.51
2M Li_2SO_4	1.397	1.168	0.229	0.68

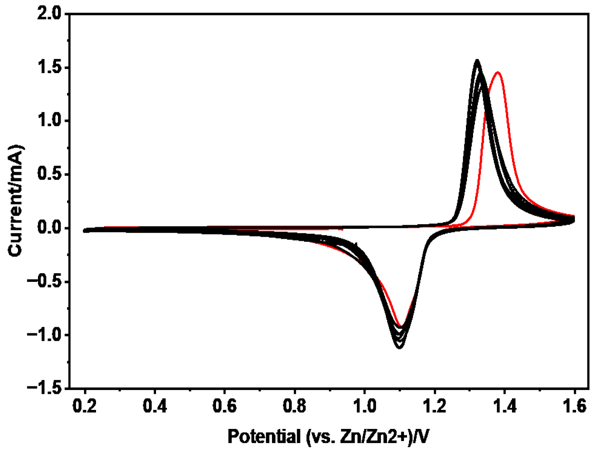

Fig. 2. CVs profiles of Zn/$LiFePO_4$ for 10 cycles, taken at a scan rate of 0.1 mV s^{-1} from 0.2V to 1.6 V (vs. Zn/Zn^{2+}) at 1M $ZnSO_4$ + 1M Li_2SO_4 electrolyte.

support effective Zn electrochemistry. Thus, CV analysis shows that the synergistic effect of Zn^{2+} and Li^+ ions is most pronounced in the 1 M $ZnSO_4$ + 1 M Li_2SO_4 electrolyte, which provides the most reversible redox behavior, minimal polarization, and balanced anodic/cathode processes, further supports the synergistic role of both cations in achieving optimal performance. Therefore, this electrolyte composition can be considered as the optimal system for further development of the application of zinc-based hybrid aqueous batteries. The electrochemical characteristics of the $LiFePO_4$ cathode in the Li^+/Zn^{2+} hybrid electrolyte were also examined to clarify the electrochemical reaction of the cathode. As Fig. 2 shows, the CV has a single pair of distinct redox peaks at around 1.1 V (reduction) and 1.3 V (oxidation) against Zn/Zn^{2+}. The peaks' shapes and positions are almost the same after each cycle, which means good reversibility and kinetic stability. These characteristics are related to the Fe^{2+}/Fe^{3+} redox pair in the reversible extraction and insertion of Li^{2+} in the olivine $LiFePO_4 \leftrightarrow FePO_4$ attice. The lack of further redox peaks proves that there are no further redox reactions involving multivalent Zn^{2+} insertion or conversion-type reactions at the cathode [33]. In line with CV results, the galvanostatic charge-discharge profiles (Fig. 4) are flat and symmetric plateaus at approximately 1.2 V, which is typical of the two-phase $LiFePO_4$/$FePO_4$ transition [34]. The plateau potential and shape are highly reversible and structurally stable with repeated Li^+ intercalation/deintercalation of the cathode after more than 50 cycles. The fact that the capacity remains constant at low voltage and the hysteresis is low also indicates that the redox process is not Zn^{2+} but Li^+ [35].

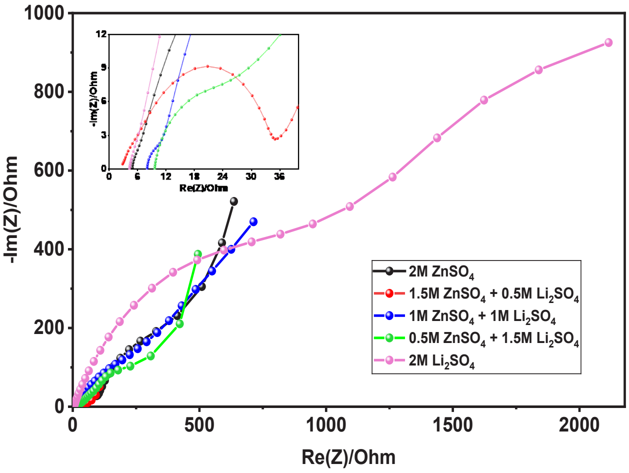

Fig. 3. Various electrolyte solutions EIS spectra.

Electrochemical impedance spectroscopy (EIS) was performed to evaluate the interfacial charge-transfer kinetics of different electrolytes. The Nyquist plots (-Im(Z) and Re(Z)) are shown in Fig. 3. The high-frequency section with the real axis corresponds to the resistance of the solution (R_s), while the diameter of the semicircle indicates the resistance of the charge transfer (R_{ct}). These parameters provide direct insight into the ionic conductivity of the electrolyte and the Zn plating/ stripping behavior. As shown in Fig. 3, the spectra vary significantly depending on the electrolyte composition. An equimolar mixture (1 M $ZnSO_4$ + 1 M Li_2SO_4) shows a relatively small semicircle corresponding to 8.91 Ω R_{ct} and 14.65 Ω R_s (Supplementary, Table S1). This indicates favorable charge transport kinetics despite the relatively high resistance of the solution, suggesting that Li^+ ions enhance the interfacial mobility of Zn^{2+} and suppress polarization. However, the 2 M $ZnSO_4$ system exhibits a R_{ct} of 9.38 Ω with a much smaller

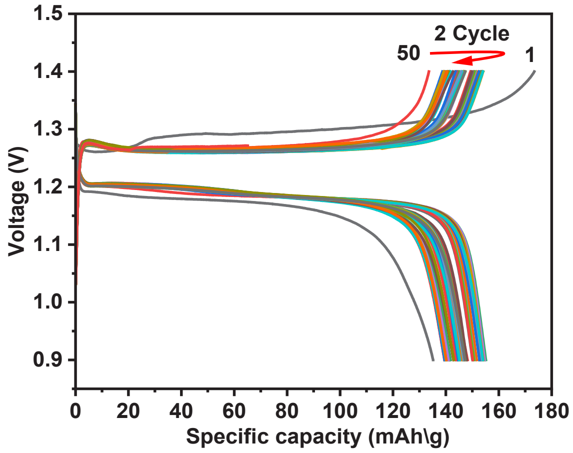

Fig. 4. Charge/Discharge profiles of Zn/$LiFePO_4$ battery at 20 mA·s^{-1}, cut of voltage 0.9-1.4 V (vs. Zn/Zn^{2+}).

R_s (4.57 Ω). Although its charge transfer resistance is close to that of an equimolar mixture, the high concentration of Zn^{2+} is associated with increased viscosity and side reactions consistent with a low turnover constant. The asymmetric formulations show divergent behavior. The 1.5 M $ZnSO_4$ + 0.5 M Li_2SO_4 system, despite a low R_s value of 2.78 Ω, gives a very high Rct of 34.31 Ω, indicating a strong interfacial resistance to charge transport. Even more surprising is the electrolyte 0.5 M $ZnSO_4$ + 1.5 M Li_2SO_4, which exhibits a very high resistance ($R_s \approx 80.32$ Ω, $R_{ct} \approx 605.50$ Ω), indicating poor ionic conductivity and slow kinetic charge transport. The 0.5 M $ZnSO_4$ + 1.5 M Li_2SO_4 system shows very high R_s (80.32 Ω) and R_{ct} (605.50 Ω), which can be explained by the following factors: first, a low concentration of Zn^{2+} reduces the availability of active ions for plating/stripping, leading to poor charge transfer; second, excess Li^+ increases the viscosity and alters the solvation structure, which may reduce ion mobility and increase bulk resistance; third, variations in ionic conductivity and interfacial charge transfer kinetics of the electrolyte formulations. The imbalance in cation ratio disrupts the optimal electric double layer formation, increasing interfacial resistance. The 2 M Li_2SO_4 system shows the worst performance, with a low solution resistance (4.22 Ω) but a very high Rct (~1456 Ω). This confirms that efficient charge transfer is not possible in the absence of a very large semicircle Zn^{2+}, making this formulation unsuitable for Zn plating/stripping. Finally, Fig. 3 clearly shows that both Rs and Rct are strongly dependent on the electrolyte composition. While the equimolar 1 M $ZnSO_4$ + 1 M Li_2SO_4 mixture shows the most balanced behavior (average Rs and lowest effective R_{ct}), asymmetric mixtures or single-salt systems lead to much higher resistance. These results are consistent with CV and galvanostatic charge-discharge results, confirming that the equimolar Zn–Li electrolyte provides the most favorable environment for Zn electrochemistry.

Galvanostatic charge-discharge measurements further confirmed the important role of electrolyte composition in electrochemical performance. The equimolar mixture (1 M $ZnSO_4$ + 1 M Li_2SO_4) exhibited a high reversible capacity (~135-158 $mAh\cdot g^{-1}$) and excellent cycling stability (Fig. 4), consistent with the reduced R_{ct} obtained by EIS. In contrast, asymmetric mixtures exhibited high initial capacity but poor retention (1.5 M $ZnSO_4$ + 0.5 M Li_2SO_4) or relatively low capacity (0.5 M $ZnSO_4$ + 1.5 M Li_2SO_4) (Supplementary Material Fig. 2b, c). The single salt 2 M $ZnSO_4$ exhibited significant polarization and capacity degradation, while 2 M Li_2SO_4 alone exhibited very low capacity (Supplementary, Figs. S2a,d), indicating the need for Zn^{2+} for reversible zinc plating/stripping. These results indicate that the optimized electrolyte formulation of 1 M $ZnSO_4$ + 1 M Li_2SO_4 achieves the best match between capacity and cycle stability, confirming its suitability for hybrid aqueous Zn-based battery systems.

The synergistic effect between Li^+ and Zn^{2+} arises from two concurrent factors: (i) regulation of solvation Li^+ ions with high hydration energy modify the Zn^{2+} solvation shell by competing for water coordination, reducing free water activity, and suppressing hydrogen evolution; and (ii) interfacial modulation Li^+ contributes to formation of a compact electric double layer on the Zn surface, which promotes uniform Zn nucleation and reduces the resistance of charge transfer. These combined effects lead to minimized corrosion current density and dendrite-free deposition in the equimolar (1 M $ZnSO_4$ + 1 M Li_2SO_4) electrolyte, confirming that this composition provides the most balanced ionic mobility and interfacial stability.

The suppression of corrosion and hydrogen evolution in the optimized electrolyte of 1 M $ZnSO_4$ + 1 M Li_2SO_4 electrolyte is mainly attributed to Li^+-induced modulation of water activity and interfacial chemistry. Specifically, Li^+ ions with strong hydration energy reduce the number of free water molecules available for the hydrogen evolution reaction (HER) by forming a more stable solvation structure around Zn^{2+}. This weakens proton reduction and mitigates local alkalization near the Zn surface. Moreover, the presence of Li^+ promotes the formation of a compact electric double layer, which inhibits direct water contact with metallic Zn and minimizes corrosion-related reactions. These effects collectively lower the corrosion current density ($j_{corr} = 0.00026$ $mA\cdot cm^{-2}$) and stabilize Zn plating/stripping behavior, as confirmed by electrochemical and morphological analyses.

The synergistic effect between Li^+ and Zn^{2+} arises from two concurrent factors: solvation regulation and interfacial modulation. Li^+ ions with strong hydration energy compete with Zn^{2+} for water coordination, thereby reducing the number of free water molecules available for hydrogen evolution and suppressing corrosion-related alkalization. Furthermore, Li^+ modifies the Zn^{2+} solvation structure, promoting the formation of $[Zn(H_2O)_4SO_4]$ complexes that exhibit enhanced ionic mobility and lower viscosity than fully hydrated $[Zn(H_2O)_6]^{2+}$ species [12]. At the electrode surface, Li^+ contributes to forming a compact electric double layer that inhibits direct contact between Zn and water, leading to uniform plating/stripping behavior and lower corrosion current density.

4. Surface morphology and composition

Before and after 50 charge/discharge cycles, the microstructural evolution of the zinc surface was examined using SEM and EDS. (Supplementary, Figs. S2) presents the morphology and elemental composition of the pristine Zn foil prior to electrochemical cycling. The SEM image shows a relatively smooth metallic surface with faint polishing marks and no visible dendritic or porous features, indicating the high initial uniformity of the electrode. Minor surface irregularities correspond to native oxide formation, as confirmed by elemental mapping and EDS spectrum. In contrast, post-cycling SEM and EDS images (Supplementary, Figs. S3) reveal pronounced differences in surface morphology depending on the electrolyte composition. In pure $ZnSO_4$ (Supplementary, Fig. S4a), the Zn surface exhibits extensive dendritic growth and corrosion pits, characteristic of uncontrolled nucleation and parasitic hydrogen evolution. The addition of a small Li_2SO_4 fraction (Supplementary, Fig. S4) partially suppresses dendrite formation but still results in non-uniform deposits and localized roughness. At higher Li_2SO_4 concentrations (Supplementary, Fig. S4c), irregular and fragmented surface features are revealed, likely due to excess Li^+ disrupting Zn^{2+} transport. At high Li_2SO_4 concentration (Supplementary, Figs. S4d), the morphology becomes more compact but highly passivated, lacks Zn deposition characteristics, confirming the absence of Zn^{2+} ions and electrochemical inactivity.

Interestingly, SEM micrographs of deposits formed in the equimolar electrolyte (1 M $ZnSO_4$ + 1 M Li_2SO_4) (Fig. 5) show a uniform, fine-grained and densely packed surface with strongly suppressed needle-like protrusions. EDS confirms Zn as the dominant element with detectable O and S signals, consistent with the presence of thin sulfate/oxide-hydroxide surface species. Although Li cannot be detected by conventional EDS as a result of its low atomic number, its influence is evident in the homogeneous nucleation and smooth morphology of the Zn deposits. This microstructural uniformity correlates well with the lowest charge-transfer resistance observed from EIS measurements and the reduced polarization seen in cyclic voltammetry and galvanostatic cycling. Together, these results confirm that the Li^+–Zn^{2+} synergistic interaction promotes uniform, dendrite-free Zn deposition and enhances long-term anode stability in aqueous hybrid electrolytes.

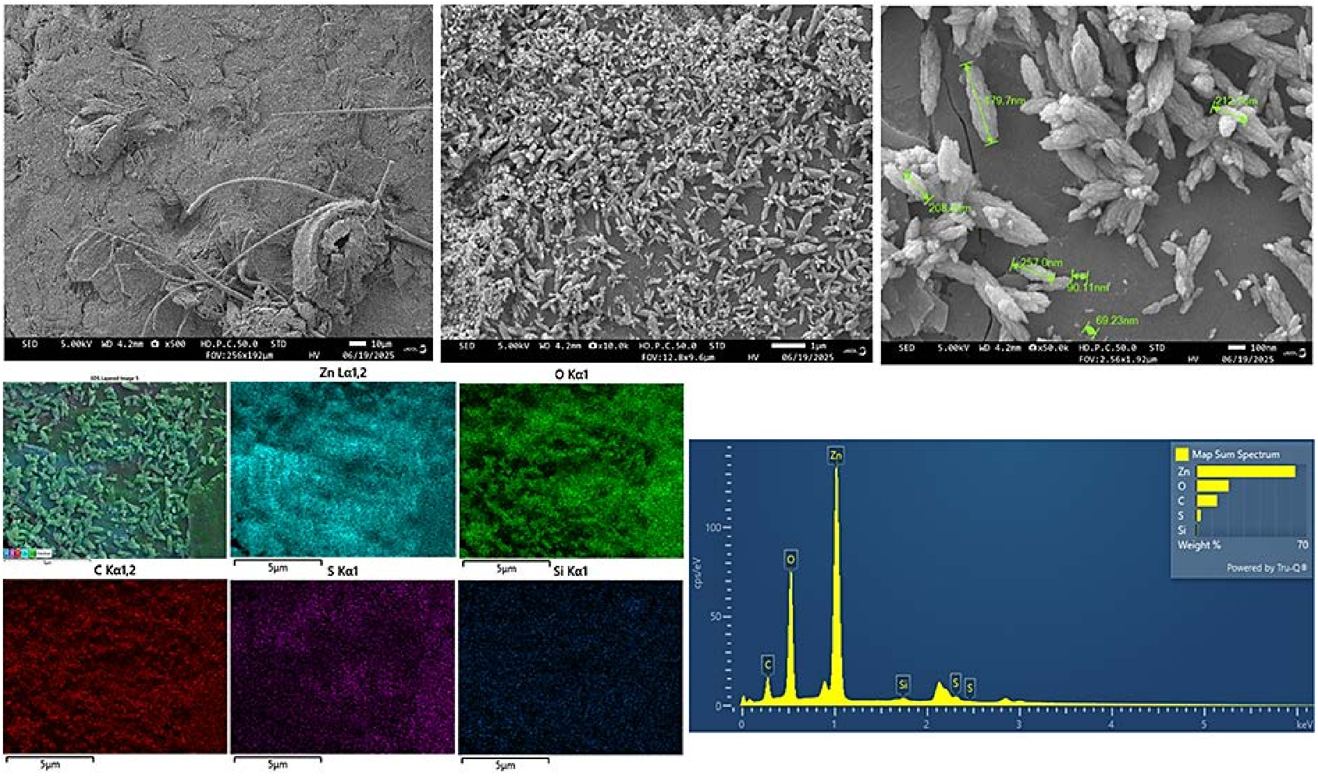

Fig. 5. SEM of after 50 cycles of charge/discharge tests.

Although in this work ex-situ structural and morphological characterization of the cycled cathode was performed and insightful observations were obtained. (Supplementary, Figs. S5) shows the SEM pictures of the $LiFePO_4$ cathode before and after 50 charge/discharge cycles in the hybrid aqueous electrolyte of $ZnSO_4$ + Li_2SO_4. The agglomerated particles of the olivine-type structure are distributed as a relatively smooth surface on $LiFePO_4$ (Fig. 5a, Supplementary Material) and have smooth morphology. After the cyclic procedure (Fig. 5b, Supplementary Material), the surface becomes rougher and displays the existence of micro-sized deposits. The analysis of the cathode used in the cycling condition through the elemental analysis (EDS) of the cathode showed that there was Zn present, which implied that a partial migration of Zn^{2+} or surface deposition was taking place during the electrochemical cycling operation.

The presence of Zn on the $LiFePO_4$ surface indicates that, in addition to Li^+ intercalation and deintercalation, there may be some involvement of Zn^{2+} at the electrode-electrolyte interface. However, there was no notable morphological degradation, including cracking or detachment, indicating that the cathode preserves its structural integrity within the hybrid electrolyte environment.

The findings align with the suggested reaction mechanism, indicating that Li^+ ions play a crucial role in the charge compensation process, while the restricted interaction of Zn^{2+} may influence surface modification after extended cycling.

Fig. 6 illustrates the XRD patterns of the $LiFePO_4$ cathode prior to and following 50 charge/discharge cycles. The diffraction peaks of the pristine sample (Supplementary, Fig. S6) are accurately indexed to olivine-type $LiFePO_4$ phase, demonstrating a high level of crystallinity and phase purity. Following the cycling process (Supplementary, Figs. S6), the primary diffraction peaks associated with $LiFePO_4$ continue to be distinctly observable and maintain their sharpness, indicating that the crystal structure is retained throughout the electrochemical cycle in the $ZnSO_4$ + Li_2SO_4 hybrid electrolyte.

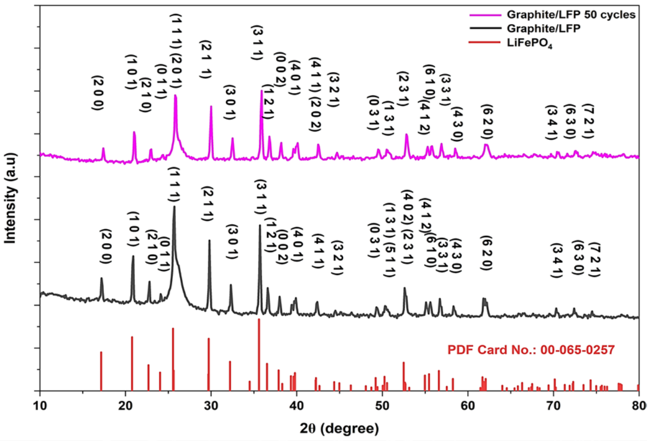

Fig. 6. XRD of LFP, before and after 50 cycles of charge/discharge tests.

No new peaks corresponding to secondary phases such as Fe_2O_3 or Li_3PO_4 are detected, confirming the structural stability of the cathode. However, a subtle reduction in the relative intensity of specific reflections could suggest minor alterations to the surface, aligning with the findings of the elemental analysis that confirm the presence of Zn after cycling.

The results indicate that although Zn^{2+} ions may adsorb or deposit on the cathode surface during cycling, they do not interfere with the $LiFePO_4$ lattice. This finding validates the favorable chemical compatibility of $LiFePO_4$ with the electrolyte system composed of $ZnSO_4$ and Li_2SO_4.

The electrochemical results obtained in this work, combined with prior literature reports on aqueous and hybrid Li^+/Zn^{2+} systems, firmly points to the fact that the main cathodic reaction is the intercalation of Li^+ into the $LiFePO_4$ framework. The improved cycling stability in the Li^+/Zn^{2+} hybrid electrolyte can be explained primarily by (i) inhibition of Zn anode corrosion and (ii) prohibition of Zn species migration or precipitation, both of which contribute to the preservation of the reversible Li^+ intercalation process in the cathode.

The obtained electrochemical data (Tafel, CV, EIS) confirm that the 1:1 Zn^{2+}:Li^+ ratio yields the lowest corrosion current density (0.00026 mA·cm^{-2}), minimal charge transfer resistance (R_{ct} = 8.91 Ω), and the most reversible redox behavior. Deviations from this ratio, such as excess Zn^{2+} or Li^+, result in poor morphology, increased interfacial resistance, and reduced reversibility. SEM analysis supports these findings, showing that only the equimolar system produces a fine-grained, stable Zn surface. Although Li^+ is not directly detected by EDS due to its low atomic number, its influence is evident in the improved morphology and electrochemical stability. These results are consistent with literature reports on dual-cation electrolytes and validate the proposed mechanism of Li^+–Zn^{2+} synergy in aqueous Zn-ion batteries.

The electrochemical, structural, and morphological results converge to reveal a consistent mechanism for the enhanced performance of the Zn‖$LiFePO_4$ system in the equimolar $ZnSO_4$ + Li_2SO_4 electrolyte. The lower corrosion current density and charge-transfer resistance observed in EIS and polarization tests correspond directly to the uniform, compact Zn morphology seen in SEM analysis. The suppression of hydrogen evolution and corrosion is further supported by the smooth surface features and absence of dendritic deposits. Simultaneously, XRD and SEM data of the $LiFePO_4$ cathode confirm the preservation of its olivine structure after cycling, indicating stable Li^+ deintercalation and the absence of parasitic reactions. Together, these findings provide a unified mechanistic understanding that Li^+ ions modulate Zn^{2+} solvation and interfacial chemistry, leading to balanced ion transport, suppressed side reactions, and long-term electrochemical stability of the hybrid aqueous Zn-ion battery.

5. Conclusion

In this study, the synergistic effects of Li^+-Zn^{2+} hybrid electrolytes on the electrochemical behavior of aqueous Zn‖$LiFePO_4$ batteries were systematically investigated. The equimolar 1 M $ZnSO_4$ + 1 M Li_2SO_4 electrolyte exhibited the lowest corrosion current density (0.00026 $mA{\cdot}cm^{-2}$) and charge-transfer resistance (8.91 Ω), along with stable cycling performance and uniform dendrite-free Zn deposition. SEM and EDS analyses confirmed the suppression of corrosion and side reactions, while XRD results verified the structural integrity of the $LiFePO_4$ cathode after cycling. The combined electrochemical and structural evidence demonstrates that Li^+ regulates Zn^{2+} solvation and interfacial chemistry, leading to improved ion transport, mitigated hydrogen evolution, and enhanced overall stability. These findings provide a clear understanding of the Li^+–Zn^{2+} synergy and offer design insights for developing safe, durable, and high-performance aqueous Zn-ion batteries.

Acknowledgement

This work was supported by Research Targeted Program “Development of new technologies of materials and energy storage systems for a green economy” BR21882402 from the Ministry of Science and Higher Education of the Republic of Kazakhstan.

References (GOST)

[1]. Mahmood A., Bai Z., Wang T., et al. Enabling high-performance multivalent metal-ion batteries: current advances and future prospects //Chemical Society Reviews. – 2025.

[2]. Zhou K., Yu X., Dong X., et al. Strategies and Prospects for Engineering a Stable Zn Metal Battery: Cathode, Anode, and Electrolyte Perspectives //Accounts of Chemical Research. – 2025. – Vol. 58. – №. 4. – P. 599-611.

[3]. Jin K., Yu Y. Principles, progress, and prospects of photo-rechargeable zinc-ion batteries //Journal of Energy Chemistry. – 2025.

[4]. Zhang Y., Cao R., Ouyang C., et al. Recent progress in alkali metal (Li/Na/K) hybrid-ion batteries: pioneering the future of energy storage //Journal of Materials Chemistry A. – 2025.

[5]. Lubis A.L., Baskoro F., Lin T.H., Wong H.Q., Liou G.S., Yen H.J. Redox-Active High-Performance Polyimides as Versatile Electrode Materials for Organic Lithium-and Sodium-Ion Batteries //ACS Applied Materials & Interfaces. – 2023. – Vol. 16. – №. 37. – P. 48722-48735.

[6]. Li R., Deng R., Wang Z., et al. The challenges and perspectives of developing solid-state electrolytes for rechargeable multivalent battery //Journal of Solid State Electrochemistry. – 2023. – Vol. 27. – №. 6. – P. 1291-1327.

[7]. Sinha R., Xie X., Yang Y., et al. Failure Mechanisms and Strategies for Vanadium Oxide-Based Cathode in Aqueous Zinc Batteries //Advanced Energy Materials. – 2025. – Vol. 15. – №. 14. – P. 2404815.

[8]. Guo X., Zhang S., Hong H., Wang S., Zhu J., Zhi C. Interface regulation and electrolyte design strategies for zinc anodes in high-performance zinc metal batteries //iScience. – 2025. – Vol. 28. – №. 2.

[9]. Zhou J., Yu H., Qing P., et al. nterfacial double-coordination effect reconstructing anode/electrolyte interface for long-term and highly reversible Zn metal anodes //Journal of Colloid and Interface Science. – 2025. – Vol. 678. – P. 772-782.

[10]. Tian Z., Li G., Chen X., et al. Innovative lignin-based MOFs and COFs for biomedicine, energy storage, and environmental remediation //Advanced Composites and Hybrid Materials. – 2025. – Vol. 8. – №. 1. – P. 114.

[11]. Wang Y., Wang T., Bu S., et al. Sulfolane-containing aqueous electrolyte solutions for producing efficient ampere-hour-level zinc metal battery pouch cells //Nature Communications. – 2023. – Vol. 14. – №. 1. – P. 1828.

[12]. Rakhman D., Batyrbekuly D., Myrzakhmetov B., et al. Polyacrylamide-based hydrogel electrolyte for modulating water activity in aqueous hybrid batteries //RSC advances. – 2024. – Vol. 14. – №. 54. – P. 40222-40233.

[13]. Qiao S., Chang L., Cui Z., Wang D., Zhang W., Zhu Q. Tuning Zn-ion de-solvation chemistry with trace amount of additive towards stable Aqueous Zn anodes //Journal of Colloid and Interface Science. – 2025. – Vol. 677. – P. 462-471.

[14]. Yang C., Woottapanit P., Geng S., et al. A multifunctional quasi-solid-state polymer electrolyte with highly selective ion highways for practical zinc ion batteries //Nature Communications. – 2025. – Vol. 16. – №. 1. – P. 183.

[15]. Huang Y., Guo R., Li Z., Zhang J., Liu W., Kang F. Ultra-Stable Aqueous Zinc Anodes: Enabling High-Performance Zinc-Ion Batteries via a ZnSiF6-Derived Protective Interphase //Advanced Science. – 2024. – Vol. 11. – №. 44. – P. 2407201.

[16]. Zhu Y., Yin J., Zheng X., Emwas A.H., Lei Y., Mohammed O.F., Cui Y., Alshareef H.N. Concentrated dual-cation electrolyte strategy for aqueous zinc-ion batteries //Energy & Environmental Science. – 2021. – Vol. 14. – №. 8. – P. 4463-4473.

[17]. Li W., Wang K., Zhou M., Zhan H., Cheng S., Jiang K. Advanced low-cost, high-voltage, long-life aqueous hybrid sodium/zinc batteries enabled by a dendrite-free zinc anode and concentrated electrolyte //ACS applied materials & interfaces. – 2018. – Vol. 10. – №. 26. – P. 22059-22066.

[18]. Wu X., Wu M., Su W., Sun Y., Huang Y., et al. High-performance aqueous Zn-organic batteries enabled by Zn-K hybrid electrolyte //Journal of Power Sources. – 2025. – Vol. 644. – P. 237057.

[19]. Zhang Y., Li H., Huang S., et al. Rechargeable aqueous zinc-ion batteries in MgSO4/ ZnSO4 hybrid electrolytes //Nano-micro letters. – 2020. – Vol. 12. – №. 1. – P. 60.

[20]. Dixit M., Hajari T., Tembe B. L. The Association of Zn2+-SO42- and Mg2+-SO42- in Aqueous MgSO4/ZnSO4 Hybrid Electrolytes: Insights from All-Atom Molecular Dynamics Simulations Molecular Dynamics Simulations //arXiv preprint arXiv:2410.15309. – 2024.

[21]. Zhao S., Li C., Zhang X., et al. An advanced Ca/Zn hybrid battery enabled by the dendrite-free zinc anode and a reversible calcification/decalcification NASICON cathode //Science Bulletin. – 2023. – Vol. 68. – №. 1. – P. 56-64.

[22]. Zhou X., Ma K., Zhang Q., et al. Highly stable aqueous zinc-ion batteries enabled by suppressing the dendrite and by-product formation in multifunctional Al3+ electrolyte additive //Nano Research. – 2022. – Vol. 15. – №. 9. – P. 8039-8047.

[23]. Fu H. et al. Exploring Hybrid Electrolytes for Zn Metal Batteries //Advanced Energy Materials. – 2025. – P. 2501152.

[24]. Hao J. et al. Toward high-performance hybrid Zn-based batteries via deeply understanding their mechanism and using electrolyte additive // Advanced Functional Materials. – 2019. – Vol. 29. – №. 34. – P. 1903605.

[25]. Wei J. et al. Advanced electrolytes for high-performance aqueous zinc-ion batteries // Chemical Society Reviews. – 2024.

[26]. Kong J. et al. Highly improved aqueous Zn‖ LiMn2O4 hybrid-ion batteries using poly (ethylene glycol) and manganese sulfate as electrolyte additives //Sustainable Energy & Fuels. – 2024. – Vol. 8. – №. 4. – P. 826-836.

[27]. Zhang Y. et al. A Comparative Study of Degradation Behaviors of LiFePO4, LiMn2O4, and LiNi0.8Mn0.1Co0.1O2 in Different Aqueous Electrolytes //Journal of The Electrochemical Society. – 2024. – Vol. 171. – №. 2. – P. 020526.

[28]. Tron A. et al. Surface modification of the LiFePO4 cathode for the aqueous rechargeable lithium ion battery //ACS Applied Materials & Interfaces. – 2017. – Vol. 9. – №. 14. – P. 12391-12399.

[29]. Zhou X. et al. Gel polymer electrolytes for rechargeable batteries toward wide-temperature applications //Chemical Society Reviews. – 2024. – Vol. 53. – №. 10. – P. 5291-5337.

[30]. Li C. et al. Boosting $Li_3V_2 (PO_4)_3$ cathode stability using a concentrated aqueous electrolyte for high-voltage zinc batteries. – 2021.

[31]. Konarov A., Myrzakhmetov B., Rapikov A., Dauletbay A. Innovative hydrogel electrolytes for hybrid zinc-ion batteries//Chemical Technologies. – 2025. - No. 2(88). P. 156-164.

[32]. Zhou Z., Wang H., Yi W., Wu S., Sun X., Li J. Engineering of hydrogel electrolyte for aqueous Zn||LiFePO4 battery on subzero-temperature adaptability, long cycles and mechanical safety //Journal of Power Sources. – 2023. – Vol. 570. – P. 233066.

[33]. Liu X., Xiong W., Zheng J., Wu J., Huang B., Zhu Q., Li Y., Xiao S., Chen Q., Yang J., Yang Z. Electrochemical performance and behavior mechanism for Zn/LiFePO4 battery in a slightly acidic aqueous electrolyte //ChemSusChem. – 2022. – Vol. 15. – №. 10. – P. e202102631.

[34]. Padhi A. K., Nanjundaswamy K. S., Goodenough J. B. Phospho-olivines as positive-electrode materials for rechargeable lithium batteries // Journal of the electrochemical society. – 1997. – Vol. 144. – №. 4. – P. 1188.

[35]. Yu Y., Xie J., Zhang H., Qin R., Liu X., Lu X. High-voltage rechargeable aqueous zinc-based batteries: latest progress and future perspectives //Small Science. – 2021. – Vol. 1. – №. 4. – P. 2000066.

References

[1]. A. Mahmood, Z. Bai, T. Wang, et al. Enabling high-performance multivalent metal-ion batteries: current advances and future prospects, Chem.

Soc. Rev. 54 (2025) 2369-2435. https://doi.org/10.1039/D4CS00929K.

[2]. K. Zhou, X. Yu, X. Dong, et al. Strategies and prospects for engineering a stable Zn metal battery: cathode, anode, and electrolyte perspectives, Acc. Chem. Res. 58 (4) (2025) 599-611. https://doi.org/10.1021/acs.accounts.4c00776.

[3]. K. Jin, Y. Yu. Principles, progress, and prospects of photo-rechargeable zinc-ion batteries, J. Energy Chem. 104 (2025) 382-396. https://doi.org/10.1016/j.jechem.2024.12.058.

[4]. Y. Zhang, R. Cao, C. Ouyang, et al. Recent progress in alkali metal (Li/Na/K) hybrid-ion batteries: pioneering the future of energy storage, J. Mater. Chem. A. 13 (2025) 3973-3990. https://doi.org/10.1039/D4TA06190J.

[5]. A.L. Lubis, F. Baskoro, T.H. Lin, et al. Redox-active high-performance polyimides as versatile electrode materials for organic lithium- and sodium-ion batteries, ACS Appl. Mater. Interfaces. 16 (2023) 48722-48735. https://doi.org/10.1021/acsami.3c10722.

[6]. R. Li, R. Deng, Z. Wang, et al. The challenges and perspectives of developing solid-state electrolytes for rechargeable multivalent battery, J. Solid State Electrochem. 27 (2023) 1291-1327. https://doi.org/10.1007/s10008-023-05426-9.

[7]. R. Sinha, X. Xie, Y. Yang, et al. Failure mechanisms and strategies for vanadium oxide-based cathode in aqueous zinc batteries, Adv. Energy Mater. 15 (2025) 2404815. https://doi.org/10.1002/aenm.202404815.

[8]. X. Guo, S. Zhang, H. Hong, et al. Interface regulation and electrolyte design strategies for zinc anodes in high-performance zinc metal batteries, iScience. 28 (2025) 111751. https://doi.org/10.1016/j.isci.2025.111751.

[9]. J. Zhou, H. Yu, P. Qing, et al. Interfacial double-coordination effect reconstructing anode/electrolyte interface for long-term and highly reversible Zn metal anodes, J. Colloid Interface Sci. 678 (2025) 772-782. https://doi.org/10.1016/j.jcis.2024.09.051.

[10]. Z. Tian, G. Li, X. Chen, et al. Innovative lignin-based MOFs and COFs for biomedicine, energy storage, and environmental remediation, Adv. Compos. Hybrid Mater. 8 (2025) 1-8. https://doi.org/10.1007/s42114-024-01201-0.

[11]. Y. Wang, T. Wang, S. Bu, et al. Sulfolane-containing aqueous electrolyte solutions for producing efficient ampere-hour-level zinc metal battery pouch cells, Nat. Commun. 14 (2025) 1828. https://doi.org/10.1038/s41467-023-37524-7.

[12]. D. Rakhman, D. Batyrbekuly, B. Myrzakhmetov, et al. Polyacrylamide-based hydrogel electrolyte for modulating water activity in aqueous hybrid batteries, RSC Adv. 14 (2024) 40222-40233. https://doi.org/10.1039/d4ra07551j.

[13]. S. Qiao, L. Chang, Z. Cui, et al. Tuning Zn-ion de-solvation chemistry with trace amount of additive towards stable aqueous Zn anodes, J. Colloid Interface Sci. 677 (2025) 462-471. https://doi.org/10.1016/j.jcis.2024.08.088.

[14]. C. Yang, P. Woottapanit, et al. A multifunctional quasi-solid-state polymer electrolyte with highly selective ion highways for practical zinc-ion batteries, Nat. Commun. 16 (2025) 183. https://doi.org/10.1038/s41467-024-55656-2.

[15]. Y. Huang, R. Guo, Z. Li, et al. Ultra-stable aqueous zinc anodes: enabling high-performance zinc-ion batteries via a $ZnSiF_6$-derived protective interphase, Adv. Sci. 11 (2025) 2407201. https://doi.org/10.1002/advs.202407201.

[16]. Y. Zhu, J. Yin, X. Zheng, et al. Concentrated dual-cation electrolyte strategy for aqueous zinc-ion batteries, Energy Environ. Sci. 14 (2021) 4463-4473. https://doi.org/10.1039/D1EE01472B.

[17]. W. Li, K. Wang, M. Zhou, et al. Advanced low-cost, high-voltage, long-life aqueous hybrid sodium/zinc batteries enabled by a dendrite-free zinc anode and concentrated electrolyte, ACS Appl. Mater. Interfaces 10 (2018) 22059-22066. https://doi.org/10.1021/acsami.8b04085.

[18]. X. Wu, M. Wu, W. Su, et al. High-performance aqueous Zn-organic batteries enabled by Zn–K hybrid electrolyte, J. Power Sources 644 (2025) 237057. https://doi.org/10.1016/j.jpowsour.2025.237057.

[19]. Y. Zhang, H. Li, S. Huang, et al. Rechargeable aqueous zinc-ion batteries in $MgSO_4/ZnSO_4$ hybrid electrolytes, Nano-Micro Lett. 12 (2020) 60. https://doi.org/10.1007/s40820-020-0385-7.

[20]. M. Dixit, T. Hajari, B.L. Tembe. The association of Zn^{2+}-SO_4^{2-} and Mg^{2+}-SO_4^{2-} in aqueous $MgSO_4/ZnSO_4$ hybrid electrolytes: insights from all-atom molecular dynamics simulations, arXiv preprint (2024). https://doi.org/10.48550/arXiv.2410.15309.

[21]. S. Zhao, C. Li, X. Zhang, et al. An advanced Ca/Zn hybrid battery enabled by the dendrite-free zinc anode and a reversible calcification/decalcification NASICON cathode, Sci. Bull. 68 (2023) 56-64. https://doi.org/10.1016/j.scib.2022.12.020.

[22]. X. Zhou, K. Ma, Q. Zhang, et al. Highly stable aqueous zinc-ion batteries enabled by suppressing the dendrite and by-product formation in

multifunctional Al^{3+} electrolyte additive, Nano Res. 15 (2022) 8039-8047. https://doi.org/10.1007/s12274-022-4419-y.

[23]. H. Fu, S. Huang, C. Wang, et al. Exploring hybrid electrolytes for Zn metal batteries, Adv. Energy Mater. 15 (2025) 2501152. https://doi.org/10.1002/aenm.202501152.

[24]. J. Hao, J. Long, B. Li, et al. Toward high performance hybrid Zn based batteries via deeply understanding their mechanism and using electrolyte additive, Adv. Funct. Mater. 29 (34) (2019) 1903605. https://doi.org/10.1002/adfm.201903605.

[25]. J. Wei, P. Zhang, J. Sun, et al. Advanced electrolytes for high performance aqueous zinc ion batteries, Chem. Soc. Rev. 53 (2024) 10335-10369. https://doi.org/10.1039/D4CS00584H.

[26]. J. Kong, H. Guo, Y. Li, et al. Highly improved aqueous Zn||$LiMn_2O_4$ hybrid ion batteries using bi-salt ($ZnSO_4$/Li_2SO_4) electrolyte with PEG/$MnSO_4$ additives, Sustain. Energy Fuels 8 (2024) 826-836. https://doi.org/10.1039/D3SE01295F.

[27]. Y. Zhang, et al. Comparative degradation of LFP/LMO/NMC in aqueous electrolytes, J. Electrochem. Soc. (2024). https://doi.org/10.1149/1945-7111/ad24c0.

[28]. A. Tron, Y.N. Jo, S.H. Oh, et al. Surface modification of the $LiFePO_4$ cathode for the aqueous rechargeable lithium-ion battery (AlF_3 coating), ACS Appl. Mater. Interfaces 9 (14) (2017) 12391-12399. https://doi.org/10.1021/acsami.6b16675.

[29]. X. Zhou, Y. Zhou, L. Yu, et al. Gel polymer electrolytes for wide-temperature rechargeable batteries (review), Chem. Soc. Rev. 53 (2024) 5291-5337. https://doi.org/10.1039/D3CS00551H.

[30]. C. Li, et al. Boosting $Li_3V_2(PO_4)_3$ cathode stability using a concentrated aqueous electrolyte (Li^+/Zn^{2+}), Chem. Commun. (2021).

[31]. A. Konarov, B. Myrzakhmetov, A. Rapikov, et al. Innovative hydrogel electrolytes for hybrid zinc-ion batteries, Chem. Technol. 2(88) (2025) 156-164. https://doi.org/10.55956/PXTX1347.

[32]. Z. Zhou, H. Wang, W. Yi, et al. Engineering of hydrogel electrolyte for aqueous Zn||$LiFePO_4$ battery on subzero-temperature adaptability, long cycles and mechanical safety, J. Power Sources 570 (2023) 233066. https://doi.org/10.1016/j.jpowsour.2023.233066.

[33]. X. Liu, W. Xiong, J. Zheng, et al. Electrochemical performance and behavior mechanism for Zn/$LiFePO_4$ battery in a slightly acidic aqueous electrolyte, ChemSusChem 15 (2022) e202102631. https://doi.org/10.1002/cssc.202102631.

[34]. A.K. Padhi, et al. Phospho-olivines as positive-electrode materials for rechargeable lithium batteries, J. Electrochem. Soc. 144 (1997) 1188. https://doi.org/10.1149/1.1837571.

[35]. Y. Yu, J. Xie, H. Zhang, et al. High-voltage rechargeable aqueous zinc-based batteries: latest progress and future perspectives, Small Sci. 1 (2021) 2000066. https://doi.org/10.1002/smsc.20200006.

About the Authors

A. Dauletbay – PhD, Senior Researcher, National Laboratory Astana, Nazarbayev University, Astana, Kazakhstan
E-mail: akbar.dauletbay@nu.edu.kz
ORCID: https://orcid.org/0000-0003-0157-1449

B. Myrzakhmetov – PhD, Senior Researcher, National Laboratory Astana, Nazarbayev University, Astana, Kazakhstan
E-mail: bauyrzhan.myrzakhmetov@nu.edu.kz
ORCID: https://orcid.org/0000-0002-6828-0649

L. Rakhymbay – PhD, Researcher, National Laboratory Astana, Nazarbayev University, Astana, Kazakhstan
E-mail: rakhymbay.lunara@nu.edu.kz
ORCID: https://orcid.org/0000-0002-7924-837X

L. Birles – bachelor, student, Faculty of Chemistry and Chemical Technology, Al-Farabi Kazakh National University, Almaty, Kazakhstan
E-mail: birleslatifa04@gmail.com

Sh. Bileimova – bachelor, student, Faculty of Chemistry and Chemical Technology, Al-Farabi Kazakh National University, Almaty, Kazakhstan
E-mail: shugyla1609@gmail.com

K. Kudaybergenov – Associate Professor, Department of Materials Science, Nanotechnology and Engineering Physics, Satbayev University, Almaty, Kazakhstan
E-mail: k.kudaibergenov@satbayev.university
ORCID: https://orcid.org/0000-0002-5444-0314

A. Konarov – PhD, Associate Professor, Department of Chemical and Materials Engineering, School of Engineering and Digital Sciences, Nazarbayev University, Astana, Kazakhstan
E-mail: aishuak.konarov@nu.edu.kz
ORCID: https://orcid.org/0000-0001-9352-8602

Синергетическое влияние гибридных электролитов Li^+–Zn^{2+} на подавление коррозии и электрохимические характеристики водных аккумуляторов Zn||$LiFePO_4$

А. Дәулетбай[1*], Б. Мырзахметов[1], Л. Рахымбай[1], Л. Бірлес[2], Ш. Әлиакбар[2], К. Кудайбергенов[3], А. Қонаров[4*]

[1]National Laboratory Astana, Назарбаев Университет, пр. Кабанбай батыра, 53, Астана, Казахстан
[2]Факультет химии и химической технологии, Казахский национальный университет им. аль-Фараби,
пр. аль-Фараби, 71, Алматы, Казахстан
[3]Кафедра Материаловедение, нанотехнологии и инженерная физика, Сатбаев университет, ул. Сатпаева, 22а,
Алматы, Казахстан
[4]Кафедра химической и материаловедческой инженерии, Школа инженерии и цифровых наук,
Назарбаев университет, пр. Кабанбай батыра, 53, Астана, Казахстан

АННОТАЦИЯ

Водные цинк-ионные аккумуляторы (AZIB) являются перспективными для безопасного и устойчивого хранения энергии. Однако нестабильность цинкового анода – образование дендритов, выделение водорода и коррозия – ограничивает долгосрочную производительность. В этом исследовании изучаются гибридные электролиты с различным соотношением Zn^{2+} и Li^+. Электролит 1 M $ZnSO_4$ + 1 M Li_2SO_4 продемонстрировал самую низкую плотность тока коррозии (0,00026 мА·см$^{-2}$), сниженное сопротивление переносу заряда (R_{ct} = 8,91 Ом) и стабильную производительность циклирования (135-158 мАч/г за 50 циклов). Электрохимический и морфологический анализы подтвердили равномерное осаждение Zn без дендритов. Эти результаты подчеркивают синергетический эффект гибридных электролитов Li^+–Zn^{2+} в повышении производительности AZIB.

Ключевые слова: водные цинк-ионные аккумуляторы, дендриты, литий-железо-фосфат, гибридный электролит, Zn-анод, анодное растворение, гальваническое осаждение.

Li^+–Zn^{2+} гибридті электролиттердің Zn||$LiFePO_4$ сулы аккумуляторларының коррозиясын басуына және электрохимиялық өнімділігіне синергетикалық әсерлері

А. Дәулетбай[1*], Б. Мырзахметов[1], Л. Рахымбай[1], Л. Бірлес[2], Ш. Әлиакбар[2], К. Кудайбергенов[3], А. Қонаров[4*]

[1]National Laboratory Astana, Назарбаев Университеті, Қабанбай батыр даңғылы 53, Астана, Қазақстан
[2]Химия және химиялық технология факультеті, Әл-Фараби атындағы Қазақ ұлттық университет, Әл-Фараби д. 71, Алматы, Қазақстан
[3]Материалтану, нанотехнология және инженерлік физика кафедрасы, Сатбаев университеті, Сатбаев к., 22а, Алматы, Қазақстан
[4]Химиялық және материалды инженерия кафедрасы, Инженерлік және цифрлық ғылымдар мектебі, Назарбаев Университеті, Астана, Қазақстан Назарбаев Университеті, Қабанбай батыр д., 53, Астана, Қазақстан

АҢДАТПА

Сулы мырыш-иондық батареялар (AZIBs) қауіпсіз және тұрақты энергияны сақтау үшін ерекше маңызды болып табылады. Дегенмен, мырыш анодының тұрақсыздығы, дендриттің түзілуі, сутегінің бөлінуі, коррозияның болуы ұзақ мерзімді өнімділікті шектейді. Бұл зерттеу Zn^{2+} және Li^+ иондарының қатынасы әртүрлі гибридті электролиттерді зерттейді. 1 M $ZnSO_4$ + 1 M Li_2SO_4 электролиті коррозияға қарсы токтың ең төменгі тығыздығын (0,00026 мА·см$^{-2}$) тудыра отырып, заряд тасымалдау кедергісін төмендетті (R_{ct} = 8,91 Ом) және тұрақты цикл өнімділігін (50 циклден астам 135-158 мАч/г) көрсетті. Электрохимиялық және морфологиялық талдаулар біркелкі, дендриттерсіз Zn шөгіндісін растады. Бұл нәтижелер AZIB өнімділігін арттырудағы Li^+–Zn^{2+} гибридті электролиттерінің синергиялық әсерін көрсетеді.

Түйін сөздер: сулы мырыш-иондық аккумуляторлар, дендриттер, литий темір фосфаты, гибридті электролит, Zn анод, анодтық еру, гальваникалық тұндыру.